



Erosional response to land abandonment in rural areas of Western Europe during the Anthropocene: A case study in the Massif-Central, France

Anthony Foucher, O. Evrard, Clément Chabert, Olivier Cerdan, Irène Lefèvre,
Rosalie Vandromme, Sebastien Salvador-Blanes

► To cite this version:

Anthony Foucher, O. Evrard, Clément Chabert, Olivier Cerdan, Irène Lefèvre, et al.. Erosional response to land abandonment in rural areas of Western Europe during the Anthropocene: A case study in the Massif-Central, France. *Agriculture, Ecosystems & Environment*, 2019, 284, pp.106582. <10.1016/j.agee.2019.106582>. <hal-02377281>

HAL Id: hal-02377281

<https://hal.science/hal-02377281v1>

Submitted on 25 May 2020

HAL is a multi-disciplinary open access archive for the deposit and dissemination of scientific research documents, whether they are published or not. The documents may come from teaching and research institutions in France or abroad, or from public or private research centers.

L'archive ouverte pluridisciplinaire **HAL**, est destinée au dépôt et à la diffusion de documents scientifiques de niveau recherche, publiés ou non, émanant des établissements d'enseignement et de recherche français ou étrangers, des laboratoires publics ou privés.



HAL Authorization

**Erosional response to land abandonment in rural areas of Western Europe
during the Anthropocene: a case study in the Massif-Central, France**

Anthony Foucher ^(1,2), Olivier Evrard ⁽¹⁾, Clément Chabert ^(1,3), Olivier Cerdan ⁽³⁾, Irène
Lefèvre ⁽¹⁾, Rosalie Vandromme ⁽³⁾, Sébastien Salvador-Blanes ⁽²⁾

⁽¹⁾ Laboratoire des Sciences du Climat et de l'Environnement, (LSCE), UMR 1572
(CEA/CNRS/UVSQ) – Bâtiment 714, Ormes des Merisiers, F-91191, Gif-sur-Yvette Cedex, France

⁽²⁾ Laboratoire GéoHydrosystèmes Continentaux (GéHCO), E.A 6293, Université F. Rabelais de
Tours, Faculté des Sciences et Techniques, Parc de Grandmont, 37200 Tours, France

⁽³⁾ Département Risques et Prévention, Bureau de Recherches Géologiques et Minières (BRGM), 3
avenue Claude Guillemin, 45060 Orléans, France

Abstract

Abandonment of agricultural land is widespread in many developed countries. These surfaces are projected to increase significantly worldwide during the 21st century. Identifying potential relationships between land abandonment and soil erosion dynamics over the long term (100 years) is therefore essential for predicting the environmental consequences of this extensive land use change. Accordingly, sediment cores were collected in two highland catchments of central France in order to reconstruct the change of sediment delivery during the last century. The results showed a substantial decline (71-78%) of rural population in both sites since 1900. This decrease occurred simultaneously with a sharp decline (85-95%) of the surface of arable land: previously cultivated areas were mainly converted into forests as the result of natural and anthropogenic processes. Consequently, sediment deliveries significantly decreased (75-99%) in both catchments. These trends were nevertheless interrupted by the implementation of afforestation works between 1945 and 1970 in one of the catchments. During these works, erosion rates increased three-fold because of extensive soil disturbance, and sediment delivery stabilized only 15 years after the onset of these management operations. Overall, this study demonstrates the long-term effect of land abandonment on soil erosion, which supplements the more widely reported acceleration trend of soil erosion because of agricultural intensification.

Keywords: land use change, afforestation, erosion decrease, highland catchment, depopulation

1. Introduction

Human activities have induced major land use changes during the 20th century worldwide (Foley et al., 2005). Natural landscapes were often converted for practicing intensive agriculture (Antrop, 2005). At many places, the drainage network across the landscape was strongly modified, with the design of streams, ditches, tile drain networks, irrigation systems and the development of landscape planning (Feder and Umali, 1993). These changes in management resulted in the significant increase in the average farm size, mainly in developed countries, and in the expansion of the agricultural areas at the expense of wetlands, forested and drier areas (Klein Goldewijk et al., 2016).

In contrast, economically unproductive areas were increasingly abandoned or reforested as a result of natural or anthropogenic processes. According to the literature, land abandonment mainly occurred in developed countries (Queiroz et al., 2014). During the 20th century, land abandonment was mainly reported from North America, the former Soviet Union and, to a lower extent, from Europe, Japan, Australia and China since the 1960s (Cramer et al., 2008). Land abandonment may result from the combination of various drivers including environmental (e.g. decline of soil fertility and productivity), social (e.g. depopulation in rural areas), economical (e.g. agriculture globalization, adjustment to the open-market) and political factors (Cramer et al., 2007; Lesiv et al., 2018).

The relationship between soil erosion and land use change is well documented in intensive agricultural areas (Boardman and Poesen, 2006; Kosmas et al., 1997), but very few records are available to quantify the link between landscape abandonment and soil erosion during the last century (e.g. Arnaez et al., 2011). However, the investigation of this issue is of paramount importance as the total area of farmland abandoned during the 20th century was estimated to 8-10% of the cultivated areas in the world in 2012 (Campbell et al., 2008), (i.e. 1.5 million km² (Navin Ramankutty and Foley, 1999). Furthermore, the surface area of

abandoned lands is projected to further significantly increase during the 21th century (Keenleyside and Tucker, 2010).

In this context of projected increase of abandoned land, a better understanding of the links occurring between landscape characteristics, land use change and sediment delivery is required. Among most of the studies that investigated these relationships, their analyses were based on model applications, field observations and they were mainly conducted in specific areas. Among these regions, Eastern Europe and Mediterranean area were the most investigated (e.g. García-Ruiz and Lana-Renault, 2011; Rodrigo-Comino et al., 2018). In particular, studies were conducted on Mediterranean terraces (Koulouri and Giourga, 2007; Lesschen et al., 2008), desertification processes (Hill et al., 2008), carbon sequestration (Novara et al., 2017; Schierhorn et al., 2013) or again on the impact of land abandonment on biodiversity and ecology (Plieninger et al., 2014; Queiroz et al., 2014).

The temporal window covered by the available studies is generally relatively short as they were often restricted to the last 40-50 years (Lasanta et al., 2017), mainly because of a lack of past land use information (e.g. aerial imagery).

To the best of our knowledge, there have been few attempts – if any – to reconstruct these relationships continuously during the Anthropocene in abandoned highland areas through the analysis of sedimentary sequences. Although the analysis of sediment cores is a powerful technique to reconstruct continuous and high resolution information on sediment inputs and erosion rates in ungauged catchments (Dearing and Jones, 2003), these approaches were almost exclusively conducted in ponds and lakes draining intensive agricultural environments during the last century (Foucher et al., 2017; Heathcote et al., 2013). Many studies were also conducted in high altitude lakes to reconstruct the processes that occurred during the entire Holocene (Bajard et al., 2016; Giguet-Covex et al., 2011), and they therefore investigated very different processes.

In the current research, sedimentary sequences were collected in two contrasted highland catchments of central France (Massif Central). These sites were selected in order to reconstruct the impact of land abandonment induced by depopulation on sediment delivery during the Anthropocene. Overall, the objective of the current project was to better understand the links between rural depopulation, land use change and the evolution of sediment delivery.

2. Sites and methods

2.1 Study sites

Two study sites representative of those contrasted trends of land cover change were selected across the Loire River basin (117,500 km²) - (Fig. 1). Both catchments are located in the low mountain range area of the Massif Central (average elevation: 714m a.s.l; peak: 1885 m a.s.l).

Prugnolas Catchment description

The Prugnolas site (45.868518N, 1.902714E) is a 7.8km² headwater catchment located on the southwestern edge of the Loire river basin (Fig. 1). The distribution of the soil types in the catchment follows that of the two main morphological areas corresponding to the leucogranitic slopes and the talwegs. On the leucogranitic slopes, the main soils are epileptic Umbrisols developed on leucogranite on the upper slopes, hyperdystric cambic Umbrisols developed on weathered leucogranite on the lower slopes and hyperdystric Cambisols developed on colluvium on the toeslopes. Within the thalwegs, soils are mainly fibric or sapric Histosols and Gleysols (INRA, 2015; IUSS Working Group WRB, 2015). The climate of this region is humid and oceanic: average annual precipitation amounts to around 1550 mm. Elevation ranges between 660 and 830 m a.s.l, with an average slope of 12%. Current

land use is mainly dominated by forests (82%), followed by natural grassland and managed grassland (16%).

The catchment's river network drains into a pond created in 1645 A.D at the outlet. This 1.8ha north-south oriented water body is a shallow environment (average water depth 0.65m) with a maximal water depth of 1.5m close to the dam. To the best of our knowledge, dredging operations were never conducted in this pond during the 20th century, although it was emptied on two occasions, i.e. in 1971 and in 1978.

Malaguet Catchment description

The Malaguet site (45.250578N, 3.713049E) is a small headwater catchment (3.7km²) located along the southern edge of the Loire River basin (Fig.1) Soils are underlain by a mix of hyperdystric Cambisols (IUSS Working Group WRB, 2015). Elevation ranges between 1025 and 1127m a.s.l, with a mean slope of 7.5%. Average annual rainfall in this area amounts to 796mm, which is characteristic of a temperate continental climate. Current land use is dominated by forests (71%) and grassland (13%).

The 2.7-km long river network drains into a medieval pond (1381AD) of 20.5ha at the catchment outlet. This northwestern-southeastern oriented water body has an average depth of 2.8m with a maximal water depth of 4.4m close to the dam, in the southeastern part (Fig. 1). To the best of our knowledge, this pond was never drained during prolonged periods.

2.2 Materials and methods

A 77 cm-long sediment core [43MA1703] was collected at 3m depth in the central part of the Malaguet lake and a 70 cm-long sediment core [23PR1701] was retrieved in the deepest part (0.9cm depth) of the Prugnolas pond. Sampling locations were selected in order to be representative of those sedimentary inputs at both sites. Core collection was performed using a floating platform and an Uwitec gravity corer equipped with a 90 mm PVC liner (Fig. 1).

Sample locations and bathymetric data were collected using a Garmin *Echomaps* depth sounder.

Laboratory analyses

Relative sediment density was recorded every 0.6mm along the sediment sequences using Computer Tomography (CT-scan) images obtained using those facilities (Siemens Somatom 128 Definition AS scanner) available at the CIRE platform (Surgery and Imaging for Research and Teaching; INRA Val de Loire, France). Relative density values were extracted from the scanner images using the free software ImageJ (Schneider et al., 2012). The relative values of density were calibrated by measuring the absolute dry bulk density (g.cm^{-3}) in 25 samples collected randomly along the core.

X-Ray Fluorescence (XRF) measurements were obtained with an Avaatech core scanner (EPOC Laboratory, Bordeaux University, France). High density records (every 0.5mm) provided relative information on the sediment geochemical content (expressed in counts by second (cps)). The K/Ca ratio characterizing the evolution of the contribution of terrigenous material to the sediment was calculated for both ponds (Croudace and Rothwell, 2015).

Sediment core dating

The chronology of sediment accumulation was established for both sites using the measurements of excess Lead-210 ($^{210}\text{Pb}_{\text{ex}}$) and Caesium-137 (^{137}Cs) in 32 samples (respectively 15 and 17 samples for the Prugnolas and Malaguet sites) of dried sediment (~10g). These gamma spectrometry measurements were obtained with the very low background GeHP detectors available at the Laboratoire des Sciences du Climat et de l'Environnement (Gif-sur-Yvette, France). Radionuclide activities were decay-corrected to the sampling date (Evrard et al., 2016b).

Ages were determined using the Constant Rate of Supply model (CRS) (Appleby and Oldfield, 1978). This model assumes variations in the rate of sediment accumulation despite a constant rate of $^{210}\text{Pb}_{\text{ex}}$ from the atmospheric fallout. The age model based on $^{210}\text{Pb}_{\text{ex}}$ records was validated through the identification of ^{137}Cs peaks in the sediment sequences, as two main sources supplied this artificial radionuclide in soils and sediment of Western Europe, i.e. thermonuclear weapons testing (with an emission peak in 1963), and the Chernobyl accident in 1986. Dating of the Prugnolas pond sediment core (23-PR-1701) is described in details in Foucher et al. (in prep).

Calculation of mass accumulation rates

Mass accumulation rate (MAR expressed in $\text{g.cm}^{-2}.\text{yr}^{-1}$) used to quantify the mass of sediment deposited for each time and surface unit was calculated as follows:

$$\text{MAR} [\text{g.cm}^{-2}.\text{yr}^{-1}] = \text{SAR} \times \text{DBD}$$

DBD corresponds to the dry bulk density (g.cm^{-3}) estimated with the ultra-high resolution calibrated CT-Scan data. SAR, expressed in cm.yr^{-1} , corresponds to the sediment accumulation rate estimated with the corrected CRS age model. This equation provides the total flux of material deposited in the reservoir, including both the production of organic material within the lake and the supply of terrigenous material from the catchment.

Evolution of land use and population

Past land use was reconstructed based on digitized aerial images and statistical records available from the French agricultural census. For the Malaguet site, eight series of aerial images taken in 1948, 1955, 1967, 1977, 1985, 1995, 2005 and 2013 were available. For the Prugnolas catchment, five series were retrieved (in 1950, 1968, 1972, 1979, 2010). Only 5 land use classes, easily identified on the pictures, were documented: water bodies, forests, arable land, grassland and urban settlements. Additional data on the land cover were derived

from the agricultural census (e.g. dominant crop types, discrimination between permanent and temporary grassland). These data were available in 1955, 1970, 1979, 1988, 2000 and 2010. Both datasets were combined to obtain a continuous time series during the 1948-2010 period.

In addition, the evolution of population in both catchments was reconstructed for the 1901-2015 period, based on those French demographic censuses conducted every 6 years. Data were only lacking for those World War periods between 1914-1918 and 1939-1945.

Statistical analyses

The Mann-Kendall non-parametric test (MK-test) was used for detecting monotonic trends in temporal series (Warren and Gilbert, 1988) and it confirmed the occurrence of monotonic upward or downward trends of a given variable throughout time (with a p -value level of 0.05). Trends can be positive, negative or non-null.

Then, the non-parametric homogeneity test (Buishand test) was used for detecting the occurrence of changes in temporal series (Buishand, 1982). Buishand test with a p -value <0.05 indicated a non-homogenous temporal trend between two periods.

Finally, the Mann-Whitney (MW-test) non-parametric test was used for detecting statistical differences between two sets of variables. MW-tests with a p -value <0.05 indicate a statistical difference between the variables.

3. Results

3.1 Evolution of population

Analysis of the demographic data showed the occurrence of a constant decrease of population in both catchments. These trends were statistically significant (MK test; p -value $<0,001$) – (Fig. 2). In Prugnolas, the population decreased from 1002 inhabitants in 1901 to 218 in 2015, corresponding to a decline of 78%. The Buishand test (p -value $<0,001$) indicates the occurrence of two periods of significant change during this period, respectively in 1918

and in 1984. For the Malaguet catchment, similar observations were made. Population declined by 71%, from 1402 inhabitants in 1901 to 399 in 2015. As for the Prugnolas catchment, the Buishand test identified two periods of significant change, in 1916 and in 1979.

These values illustrate the progressive depopulation of both catchments during the 20th century. This rural depopulation accelerated after WWI and continued until the 1980s. The trends found in these rural areas are in opposition with those observed at the national level, with a significant increase of the total population in France after WWII (Fig. 2).

3.2 Evolution of land use

In the Prugnolas catchment, the proportion of agricultural land (both cropland and grassland) decreased throughout time (MK-test p -value $<0,001$) – (Fig. 3). The surface dedicated to agricultural production (livestock and cereal production) decreased by 76% in 60 years. In particular, the cropland surface area which amounted to 7.3% of arable land in 1950, decreased to only 0.4% in 2010 (95%-decrease). During the same period, grassland surface decreased by 74%. Agricultural land was mainly replaced with forest. Forested and abandoned grassland characterized by the regrowth of trees increased by 173% between 1950 and 2010 (covering respectively 30% of the catchment surface area in 1950 and 82% in 2010). Figure 4 shows the temporal evolution of the spatial pattern of forested surfaces in this catchment during the second half of the 20th century. The Buishand test indicates the stabilization of these land use proportions from 1970 onwards.

For the Malaguet catchment, the proportion of agricultural land (cropland and grassland) also decreased throughout time (MK-test p -value $<0,001$). The surface dedicated to agricultural production was divided by 3 between 1948 and 2010 (decreasing from 45 to 15% of the catchment surface) - (Fig. 3). In particular, cropland areas decreased from 85% in 55

years (covering respectively 13% of the surface in 1955 against 2% nowadays). Cropland was mainly replaced with permanent/temporal grasslands. The surface of the permanent area under grass increased respectively from 67% to 88% of the agricultural surface during the second half of the 20th century. In parallel to the decline of agricultural land, the proportion of forested areas rose by 67% between 1948 and 2010 (increasing respectively from 43% to 72% of the catchment surface). This increase illustrates the occurrence of reforestation since 1955 (p -value <0,05) – (Fig. 3).

Both catchments showed the progressive encroachment of the landscape with woodland during the second part of the 20th century, mainly through afforestation and/or conversion of cropland into grassland or unmanaged forests.

3.3 Sediment dating

Dating of the Prugnolas sediment sequence was detailed in Foucher et al. (in prep). This archive covers the sedimentation processes that occurred until 1900. ¹³⁷Cs activity was detected from 45.5 cm depth (4.2 ± 0.2 Bq.kg⁻¹) in the Malaguet sequence (Fig. 5). Maximal concentration in this radionuclide was recorded at 15.5 cm depth (100.3 ± 2.4 Bq.kg⁻¹). Log ²¹⁰Pb_{ex} activities significantly decreased with depth ($r^2=0.88$) – (Fig. 5). The CRS model was applied to date this sequence that deposited between 1947 and 2017. Age models based on ²¹⁰Pb_{ex} and ¹³⁷Cs were compared. The single peak of ¹³⁷Cs found was estimated to correspond to 1986 ± 1.2 years. The onset of the radiocesium deposits found at 45.5cm depth was dated to 1955 ± 2 years. Within the sequence, ²¹⁰Pb_{ex} activities showed the occurrence of two periods of decrease of this radionuclide activities, first between 38.5 and 45.5 cm depth (between 1963 and 1955) and then between 18.5 and 25.5 cm depth (corresponding to the 1981–1973 period).

3.4 Estimation of Mass Accumulation Rate (MAR) and the terrigenous fraction of sediment

Evolution of MAR in the Prugnolas pond shows a constant decrease of sediment delivery throughout time (MK test; $p < 0.001$). Sediment supply to the lake decreased from $0.4 \text{ g.cm}^{-2}.\text{yr}^{-1}$ to $0.04 \text{ g.cm}^{-2}.\text{yr}^{-1}$ between 1907 and 2017 (Fig. 6). The period of maximum sediment input was recorded between 1900 and 1913, with an average rate of $0.3 \pm 0.08 \text{ g.cm}^{-2}.\text{yr}^{-1}$. This period was followed between 1913 and 1919 by a sharp decline of those inputs (average MAR = $0.18 \pm 0.03 \text{ g.cm}^{-2}.\text{yr}^{-1}$). After the WWI, sediment delivery first increased slowly before decreasing significantly during the 1920s. From the 1960s onwards, sediment input decreased significantly from $0.1 \text{ g.cm}^{-2}.\text{yr}^{-1}$ in 1960 to $0.05 \text{ g.cm}^{-2}.\text{yr}^{-1}$ in 1965 (Fig. 6). The terrigenous fraction of sediment estimated based on the XRF data showed a similar trend as that of the total flux of sediment (MK test; <0.001). Relationship between MAR and the K/Ca ratio (used as a proxy for estimating the terrigenous fraction of sediment) was significant ($r^2=0.66$). This correlation suggests an accumulation of material produced by erosional processes occurring in the catchment. The 1900-1940 period corresponds to the period of maximal export of terrigenous material recorded in this sequence. However, during this phase, the terrigenous inputs decreased between 1908 and 1916, as observed for the MAR. From 1950 onwards, the inputs increased slowly before decreasing significantly in the early 1960s until the early 1980s. Then, the terrigenous inputs remained constant over time at a much lower level (Fig. 6).

For the Malaguet lake, MAR exhibited two distinct trends of material inputs (Fig. 7). First, the lower levels of the core (between 1951 and 1963) recorded the highest sediment input levels of the entire sequence (average MAR = $0.6 \pm 0.4 \text{ g.cm}^{-2}.\text{yr}^{-1}$). Within this large period, four specific levels were identified based on the ultra-high resolution Ct-scan data:

respectively in 1951-1953, 1954-1955, 1955-1959 and, finally, in 1961 (maximal MAR values of these levels: 1.7; 0.92; 1.1; 0.7 g.cm⁻².yr⁻¹).

Then, in the upper part of the sequence corresponding to the period from the late 1960s to 2017, constant values of MAR over time were found (average MAR for this period = 0.15 ± 0.06 g.cm⁻².yr⁻¹). From the second half of the 1950s, MAR exhibited a statically negative trend (MK test: *p*-value <0.001). Similar trends were observed for the evolution of the terrigenous fraction estimated based on the K/Ca proxy, except for the 1951-1953 period where a additional peak of this fraction was detected. K/Ca ratio was strongly correlated to the MAR values (*r*²=0.84). This positive relationship demonstrates that the sediment supply to the lake was dominated by soil erosion in the catchment.

4. Discussion

Results obtained in both catchments indicate the occurrence of a statistically significant decline of sediment delivery and terrigenous inputs to the lakes of this region throughout the 20th century. This decrease was observed during a period of major rural depopulation and land cover change representative of those observed in other remote and rural regions of France and Europe (Lasanta et al., 2017).

Sediment accumulation in the ponds decreased by 75% (Malaguet) to 99% (Prugnolas) during the study period. These results are consistent with observations made in other catchments of Eastern and Southern Europe. In Spain, farmland abandonment and land reforestation were shown to have induced a decline of 54% in sediment yields (Boix-Fayos et al., 2008). In Poland, erosion rates have decreased by 76% after land abandonment associated with depopulation (Latocha et al., 2016). The same trend was observed in Slovenia (decline of 69% of the total sediment delivery) - (Keesstra et al., 2009). However, these studies were all based on model outputs (and not on field-based observations).

In the current research, the change in sediment delivery was strongly correlated to the decrease of the arable land surfaces ($r^2=0.97$ and $r^2=0.94$, respectively for the Prugnolas and Malaguet catchments) - (Fig. 8). Similar trends were observed in model-based studies conducted across Europe (e.g. Corbelle-Rico et al., 2012; Van Rompaey et al., 2007).

Furthermore, in the current research, land abandonment was strongly correlated to the rate of depopulation ($r^2=0.91$ and 0.86 respectively for Prugnolas and Malaguet)– (Fig. 8). This corroborates previous results on the link between depopulation and land abandonment obtained in Eastern Europe or in the Mediterranean region (e.g. Kosmas et al., 2015; Pazúr et al., 2014).

The detailed chronology of population and land use change in the two catchments investigated in the current research showed that the strongest changes occurred during the post-WWII period. After 1945, a significant movement of land abandonment by farmers was observed in this rural region. Before leaving, farmers planted trees in their arable land to provide them an additional source of income. In addition of these local reforestation operations, the French authorities have financially supported afforestation programmes in many areas of the Massif-Central region. These operations mainly took place between 1945 and 1970. The physiognomy of Massif-Central landscapes drastically changed, from a dominance of bare ground areas to one of the densest forested areas in France. In addition to these afforestation works, spontaneous reforestation occurred in abandoned cropland. At the French scale, 4.5 million hectares were reforested (corresponding to 30% of the surface of French forests by 2000, i.e. 8% of the French territory) as a result of coordinated operations and natural regrowth after land abandonment between 1945 and 1999. The Massif-Central region is one of the most reforested areas in France (Dodane, 2009).

Surprisingly, in the Malaguet catchment, afforestation periods correspond to the main sediment input phases into the lake. Afforestation works were already described as a potential

factor accelerating soil erosion rates (e.g. Romero-Diaz et al., 2010). Detrital pulses detected in the Malaguet sediment core were associated with a decrease in the sediment $^{210}\text{Pb}_{\text{ex}}$ activities. This may reflect the preferential mobilization of subsoil material sheltered from atmospheric fallout and depleted in fallout radionuclides (Evrard et al., 2016a; Foucher et al., 2015; Laceby et al., 2017; Le Gall et al., 2017) during these operations and further supports the hypothesis of major landscape disturbances, which would have occurred between 1950 and 1970 in this catchment (e.g. Simms et al., 2008). After this extensive land use conversion, soil erosion rates decreased from a mean of $135 \text{ t.km}^{-2}.\text{year}^{-1}$ between 1945-1950 to a mean of $28 \text{ t.km}^{-2}.\text{year}^{-1}$ between 2000-2017. Maximal erosion rates were recorded at the onset of the different phases of afforestation within these catchments, with the occurrence of four detrital layers ($250, 240, 280$ and $210 \text{ t.km}^{-2}.\text{year}^{-1}$, estimated to have deposited in 1951-1953, 1954-1955, 1956-1959 and 1961, respectively). These layers were likely associated with the occurrence of major land use changes, or afforestation works in the area draining to the lake.

Approximately 15 years after the completion of the afforestation programmes, sediment export tended to stabilize with the widespread development of forest canopy and the hillslope stabilization (with the root growth and the increase in the soil cover by vegetation). Similar observations were made in an afforested site of Scotland (Battarbee et al., 1985). Sediment accumulation increased ten-fold during this disturbance period, and it then returned to the pre-afforestation levels after about 10 years.

In the Prugnolas catchment, afforestation works were less extensive and they mainly took place in upper catchment parts, in areas that are not well connected to the lake. Furthermore, this process mainly resulted from the natural regrowth of trees on abandoned agricultural land. Accordingly, in this context, the impact of reforestation on soil erosion rates remained low, with the exception of a slight increase of the terrigenous inputs into the lake

between 1945 and 1980. However, despite this limited increase, the sediment accumulation sequence recorded in this core illustrates the sedimentation in a lake draining a relatively undisturbed natural catchment compared to the situation observed in the Malaguet lake, where larger changes in sediment inputs were observed in response to both natural and anthropogenic changes in the drainage area.

We would like to thank the reviewer for this valuable suggestion. Comparison with studies compiling erosion rates in similar environments were added to the discussion section (LL.375-389).

In contrast to the two sites impacted by land abandonment investigated in the current research, other basins with similar initial land uses were affected by distinct soil erosion trajectories. In the UK, Foster and Lee (1999) summarized a large number of these trajectories deduced from the analysis of sedimentary sequences. For instance, sediment cores collected in the Silsden reservoir (Yorkshire) underwent a three-fold higher sediment supply in 1990 compared to that observed at the end of the 19th century. As no major change in the arable land proportion was observed in the drainage area, this accelerated sediment supply was attributed to the increased surface areas covered with grassland for both sheep and cattle grazing. A similar trend was recorded in the Elleron lake (Yorkshire) where sheep and cattle grazing have led to a two-fold increase of the sediment production during the 20th century, without any significant change in the arable land surface area. In contrast, in catchments impacted by land use change (transition from grassland to arable land) as in that of Fillingham lake (East Midlands), sediment production increased 5-fold after agricultural intensification. Similar dynamics were recorded in the Yetlhom lake (East Midlands) where grassland was massively converted into arable land (after 1921). These changes increased sediment delivery from 22 times.

In contrast to the well-documented great acceleration of soil erosion observed during the 20th century in agricultural plains (Foucher et al., 2014; N. Ramankutty and Foley, 1999), relatively few studies quantified this opposite trajectory of soil erosion decrease in response to land abandonment. The surface of abandoned land should increase across the world during the 21st century. Existing data estimated the extent of farmland abandonment in 2030 to 3-4% of the currently utilized agricultural area in Europe (corresponding to 126,000-168,000 km²) - (Keenleyside and Tucker, 2010). In Japan, official statistics estimated the total abandonment rate of cropland at 10.6% in 2010 (Osawa et al., 2015). In eastern Europe between 15 and 20% of cropland areas have been abandoned since the 1980's. In post-soviet Russia, more than 40 million hectares of arable lands were abandoned (Rosstat, 2010). In Western Europe, rate of land abandonment is estimated to 0.17% in France and 0.8% in Spain (Pointereau et al., 2008).

Return to cultivation of this abandoned land is very difficult or even not feasible for economic reasons (Corbelle-Rico and Crecente-Maseda, 2008). The two land use conversion patterns (deforestation for intensive agriculture and land abandonment) will likely not balance each other in the next future decades. Accordingly, a better quantification of the processes that occurred in these areas remains a challenge to improve estimations of the global soil erosion budget and its spatial and temporal variations.

Conclusions

The investigation of sediment accumulation in lakes provides a powerful technique for reconstructing the impact of human activities on soil erosion rates. Although lake deposits were extensively used in high altitude regions (e.g. in the Alps) for quantifying the impact of the agricultural expansion and its subsequent abandonment on soil erosion, very few records

are available to investigate the impact of these changes in remote and rural highland areas. The current research quantified the occurrence of a significant decline of sediment delivery and terrigenous inputs to the lakes of remote and rural highland areas of western Europe, throughout the 20th century. In 100 years, sediment production has decreased of 75 to 99% in these areas. This general decrease was observed during a period of major rural depopulation and the associated land cover change, with a massive conversion of arable land into forests. These results showed how complex soil erosion trajectories may be at the regional scale. These processes that are often neglected in the current soil erosion investigations should be better taken into account for improving modelling approaches and designing sustainable strategies of land use management and food security in a world in demographic expansion.

Acknowledgements

The authors are grateful to Anne Colmar, Xavier Bourrain and Jean-Noël Gautier for their technical and financial support. This work was supported by a grant from the Loire-Brittany Water Agency (METEOR project). The authors would also like to thank Jerome Vany (Office National des Forêts), Peggy Chevilley (Communauté de Commune de Bourganeuf) and Nathanaël Lefèvre (PNR Livradois-Forez) for their precious help to obtain historical data on the studied catchments. Authors also gratefully acknowledge Naresh Kumar and Anastasiia Bagaeva for their help during field surveys.

References

- Antrop, M., 2005. Why landscapes of the past are important for the future. *Landsc. Urban Plan.* 70, 21–34. <https://doi.org/http://dx.doi.org/10.1016/j.landurbplan.2003.10.002>
- Appleby, P.G., Oldfield, F., 1978. The calculation of lead-210 dates assuming a constant rate

448 of supply of unsupported ^{210}Pb to the sediment. *Catena* 5, 1–8.
449 [https://doi.org/10.1016/S0341-8162\(78\)80002-2](https://doi.org/10.1016/S0341-8162(78)80002-2)

450 Arnaez, J., Lasanta, T., Errea, M.P., Ortigosa, L., 2011. Land abandonment, landscape
451 evolution, and soil erosion in a Spanish Mediterranean mountain region: The case of
452 Camero Viejo. *L. Degrad. Dev.* 22, 537–550. <https://doi.org/10.1002/ldr.1032>

453 Bajard, M., Sabatier, P., David, F., Develle, A.L., Reyss, J.L., Fanget, B., Malet, E., Arnaud,
454 D., Augustin, L., Crouzet, C., Poulenard, J., Arnaud, F., 2016. Erosion record in Lake La
455 Thuile sediments (Prealps, France): Evidence of montane landscape dynamics
456 throughout the Holocene. *Holocene*. <https://doi.org/10.1177/0959683615609750>

457 Battarbee, R.W., Appleby, P.G., Odell, K., Flower, R.J., 1985. ^{210}Pb dating of scottish lake
458 sediments, afforestation and accelerated soil erosion. *Earth Surf. Process. Landforms*.
459 <https://doi.org/10.1002/esp.3290100206>

460 Boardman, J., Poesen, J., 2006. Soil Erosion in Europe, *Soil Erosion in Europe*.
461 <https://doi.org/10.1002/0470859202>

462 Boix-Fayos, C., de Vente, J., Martínez-Mena, M., Barberá, G.G., Castillo, V., 2008. The
463 impact of land use change and check-dams on catchment sediment yield. *Hydrol.*
464 *Process.* <https://doi.org/10.1002/hyp.7115>

465 Buishand, T.A., 1982. Some methods for testing the homogeneity of rainfall records. *J.*
466 *Hydrol.* [https://doi.org/10.1016/0022-1694\(82\)90066-X](https://doi.org/10.1016/0022-1694(82)90066-X)

467 Campbell, J.E., Lobell, D.B., Genova, R.C., Field, C.B., 2008. The global potential of
468 bioenergy on abandoned agriculture lands. *Environ. Sci. Technol.*
469 <https://doi.org/10.1021/es800052w>

470 Corbelle-Rico, E., Crecente-Maseda, R., 2008. Abandonment of agricultural land: an

471 overview of drivers and consequences. *Rev. Galega Econ.* 17.

472 Corbelle-Rico, E., Crecente-Maseda, R., Santé-Riveira, I., 2012. Multi-scale assessment and
 473 spatial modelling of agricultural land abandonment in a European peripheral region:
 474 Galicia (Spain), 1956–2004. *Land use policy* 29, 493–501.
 475 <https://doi.org/10.1016/j.landusepol.2011.08.008>

476 Cramer, V.A., Hobbs, R.J., Society for Ecological Restoration International., 2007. Old
 477 fields : dynamics and restoration of abandoned farmland, *The science and practice of*
 478 *ecological restoration*.

479 Cramer, V.A., Hobbs, R.J., Standish, R.J., 2008. What’s new about old fields? *Land*
 480 *abandonment and ecosystem assembly. Trends Ecol. Evol.*
 481 <https://doi.org/10.1016/j.tree.2007.10.005>

482 Croudace, I.W., Rothwell, R.G., 2015. Micro-XRF Studies of Sediment Cores: Applications
 483 of a non-destructive tool for the environmental sciences, *Developments in*
 484 *Paleoenvironmental Research.* <https://doi.org/10.1007/978-94-017-9849-5>

485 Dearing, J.A., Jones, R.T., 2003. Coupling temporal and spatial dimensions of global
 486 sediment flux through lake and marine sediment records. *Glob. Planet. Change* 39, 147–
 487 168. [https://doi.org/http://dx.doi.org/10.1016/S0921-8181\(03\)00022-5](https://doi.org/http://dx.doi.org/10.1016/S0921-8181(03)00022-5)

488 Dodane, C., 2009. Les nouvelles forêts du Massif Central: enjeux sociétaux et territoriaux.
 489 Ces hommes qui plantaient des résineux pour éviter la friche.

490 Evrard, O., Laceby, J.P., Huon, S., Lefèvre, I., Sengtaheuanghoung, O., Ribolzi, O., 2016a.
 491 Combining multiple fallout radionuclides (^{137}Cs , ^7Be , ^{210}Pb s) to investigate temporal
 492 sediment source dynamics in tropical, ephemeral riverine systems. *J. Soils Sediments.*
 493 <https://doi.org/10.1007/s11368-015-1316-y>

494 Evrard, O., Laceby, J.P., Onda, Y., Wakiyama, Y., Jaegler, H., Lefèvre, I., 2016b.
495 Quantifying the dilution of the radiocesium contamination in Fukushima coastal river
496 sediment (2011–2015). *Sci. Rep.* 6, 34828. <https://doi.org/10.1038/srep34828>

497 Feder, G., Umali, D.L., 1993. The adoption of agricultural innovations. A review. *Technol.*
498 *Forecast. Soc. Change.* [https://doi.org/10.1016/0040-1625\(93\)90053-A](https://doi.org/10.1016/0040-1625(93)90053-A)

499 Foley, J.A., Defries, R., Asner, G., Barford, C., Bonan, G., Carpenter, S., Chapin, F., Coe, M.,
500 Daily, G., Gibbs, H., Helkowski, J., Holloway, T., Howard, E., Kucharik, C., Monfreda,
501 C., Patz, J., Prentice, I., Ramankutty, N., Snyder, P., 2005. Global Consequences of Land
502 Use. *Science* (80-.). 309, 570–574. <https://doi.org/10.1126/science.1111772>

503 Foucher, A., Le Gall, M., Salvador blanes, S., Evrard, O., Cerdan, O., Laceby, J.P.,
504 Vandromme, R., Lefevre, I., Maniere, L., Grangeon, T., Bakyono, J.P., Desmet, M.,
505 2017. Increase of erosion source contributions to rivers and lakes (1950 2010): The case
506 of the Louroux Pond (Central France). *Houille Blanche* 2017–Decem.
507 <https://doi.org/10.1051/lhb/2017051>

508 Foucher, A., Patrick Laceby, J., Salvador-Blanes, S., Evrard, O., Le Gall, M., Lefèvre, I.,
509 Cerdan, O., Rajkumar, V., Desmet, M., 2015. Quantifying the dominant sources of
510 sediment in a drained lowland agricultural catchment: The application of a thorium-
511 based particle size correction in sediment fingerprinting. *Geomorphology.*
512 <https://doi.org/10.1016/j.geomorph.2015.09.007>

513 Foucher, A., Salvador-Blanes, S., Evrard, O., Simonneau, A., Chapron, E., Courp, T., Cerdan,
514 O., Lefèvre, I., Adriaensen, H., Lecompte, F., Desmet, M., 2014. Increase in soil erosion
515 after agricultural intensification: Evidence from a lowland basin in France. *Anthropocene*
516 7, 30–41. <https://doi.org/10.1016/j.ancene.2015.02.001>

517 García-Ruiz, J.M., Lana-Renault, N., 2011. Hydrological and erosive consequences of

518 farmland abandonment in Europe, with special reference to the Mediterranean region - A
519 review. *Agric. Ecosyst. Environ.* <https://doi.org/10.1016/j.agee.2011.01.003>

520 Giguët-Covex, C., Arnaud, F., Poulenard, J., Disnar, J.-R., Delhon, C., Francus, P., David, F.,
521 Enters, D., Rey, P.-J., Delannoy, J.-J., 2011. Changes in erosion patterns during the
522 Holocene in a currently treeless subalpine catchment inferred from lake sediment
523 geochemistry (Lake Anterne, 2063 m a.s.l., NW French Alps): The role of climate and
524 human activities. *The Holocene* 21, 651–665.
525 <https://doi.org/10.1177/0959683610391320>

526 Heathcote, A.J., Filstrup, C.T., Downing, J.A., 2013. Watershed Sediment Losses to Lakes
527 Accelerating Despite Agricultural Soil Conservation Efforts. *PLoS One* 8, e53554.
528 <https://doi.org/10.1371/journal.pone.0053554>

529 Hill, J., Stellmes, M., Udelhoven, T., Röder, A., Sommer, S., 2008. Mediterranean
530 desertification and land degradation. Mapping related land use change syndromes based
531 on satellite observations. *Glob. Planet. Change.*
532 <https://doi.org/10.1016/j.gloplacha.2008.10.005>

533 INRA, 2015. Référentiel régional pédologique du Limousin à 1/250 000e. Régions naturelles,
534 pédopaysages et sols.

535 IUSS Working Group WRB, 2015. World Reference Base for Soil Resources 2014, update
536 2015. International soil classification system for naming soils and creating legends for
537 soil maps., World Soil Resources Reports No. 106.

538 Keenleyside, C., Tucker, G., 2010. Farmland abandonment in the EU: an assessment of trends
539 and prospects. Rep. Prep. WWF, Inst. Eur. Environ. Policy.
540 <https://doi.org/10.1016/j.outlook.2010.06.002>

541 Keesstra, S.D., van Dam, O., Verstraeten, G., van Huissteden, J., 2009. Changing sediment
 542 dynamics due to natural reforestation in the Dragonja catchment, SW Slovenia. *Catena*.
 543 <https://doi.org/10.1016/j.catena.2009.02.021>

544 Klein Goldewijk, K., Beusen, A., Doelman, J., Stehfest, E., 2016. New anthropogenic land
 545 use estimates for the Holocene; HYDE 3.2. *Earth Syst. Sci. Data Discuss.* 1–40.
 546 <https://doi.org/10.5194/essd-2016-58>

547 Kosmas, C., Danalatos, N., Cammeraat, L.H., Chabart, M., Diamantopoulos, J., Farand, R.,
 548 Gutierrez, L., Jacob, A., Marques, H., Martinez-Fernandez, J., Mizara, A., Moustakas,
 549 N., Nicolau, J.M., Oliveros, C., Pinna, G., Puddu, R., Puigdefabregas, J., Roxo, M.,
 550 Simao, A., Stamou, G., Tomasi, N., Usai, D., Vacca, A., 1997. The effect of land use on
 551 runoff and soil erosion rates under Mediterranean conditions. *Catena*.
 552 [https://doi.org/10.1016/S0341-8162\(96\)00062-8](https://doi.org/10.1016/S0341-8162(96)00062-8)

553 Kosmas, C., Kairis, O., Karavitis, C., Acikalin, S., Alcalá, M., Alfama, P., Atlhopheng, J.,
 554 Barrera, J., Belgacem, A., Solé-Benet, A., Brito, J., Chaker, M., Chanda, R., Darkoh, M.,
 555 Ermolaeva, O., Fassouli, V., Fernandez, F., Gokceoglu, C., Gonzalez, D., Gungor, H.,
 556 Hessel, R., Khatteli, H., Khitrov, N., Kounalaki, A., Laouina, A., Magole, L., Medina,
 557 L., Mendoza, M., Mulale, K., Ocakoglu, F., Ouessar, M., Ovalle, C., Perez, C., Perkins,
 558 J., Pozo, A., Prat, C., Ramos, A., Ramos, J., Riquelme, J., Ritsema, C., Romanenkov, V.,
 559 Sebege, R., Sghaier, M., Silva, N., Sizemskaya, M., Sonmez, H., Taamallah, H., Tezcan,
 560 L., de Vente, J., Zagal, E., Zeiliger, A., Salvati, L., 2015. An exploratory analysis of
 561 land abandonment drivers in areas prone to desertification. *CATENA* 128, 252–261.
 562 <https://doi.org/10.1016/j.catena.2014.02.006>

563 Koulouri, M., Giourga, C., 2007. Land abandonment and slope gradient as key factors of soil
 564 erosion in Mediterranean terraced lands. *Catena*.

565 <https://doi.org/10.1016/j.catena.2006.07.001>

566 Laceby, J.P., Evrard, O., Smith, H.G., Blake, W.H., Olley, J.M., Minella, J.P.G., Owens, P.N.,
567 2017. The challenges and opportunities of addressing particle size effects in sediment
568 source fingerprinting: A review. *Earth-Science Rev.*
569 <https://doi.org/10.1016/j.earscirev.2017.04.009>

570 Lasanta, T., Arnáez, J., Pascual, N., Ruiz-Flaño, P., Errea, M.P., Lana-Renault, N., 2017.
571 Space–time process and drivers of land abandonment in Europe. *Catena*.
572 <https://doi.org/10.1016/j.catena.2016.02.024>

573 Latocha, A., Szymanowski, M., Jeziorska, J., Stec, M., Roszczewska, M., 2016. Effects of
574 land abandonment and climate change on soil erosion-An example from depopulated
575 agricultural lands in the Sudetes Mts., SW Poland. *Catena*.
576 <https://doi.org/10.1016/j.catena.2016.05.027>

577 Le Gall, M., Evrard, O., Foucher, A., Laceby, J.P., Salvador-Blanes, S., Manière, L., Lefèvre,
578 I., Cerdan, O., Ayrault, S., 2017. Investigating the temporal dynamics of suspended
579 sediment during flood events with ^7Be and ^{210}Pb xs measurements in a drained
580 lowland catchment. *Sci. Rep.* 7. <https://doi.org/10.1038/srep42099>

581 Lesiv, M., Schepaschenko, D., Moltchanova, E., Bun, R., Dürauer, M., Prishchepov, A. V.,
582 Schierhorn, F., Estel, S., Kuemmerle, T., Alcántara, C., Kussul, N., Shchepashchenko,
583 M., Kutovaya, O., Martynenko, O., Karminov, V., Shvidenko, A., Havlik, P., Kraxner,
584 F., See, L., Fritz, S., 2018. Data descriptor: Spatial distribution of arable and abandoned
585 land across former Soviet Union countries. *Sci. Data*.
586 <https://doi.org/10.1038/sdata.2018.56>

587 Lesschen, J.P., Cammeraat, L.H., Nieman, T., 2008. Erosion and terrace failure due to
588 agricultural land abandonment in a semi-arid environment. *Earth Surf. Process.*

589 Landforms. <https://doi.org/10.1002/esp.1676>

590 Novara, A., Gristina, L., Sala, G., Galati, A., Crescimanno, M., Cerdà, A., Badalamenti, E.,
591 La Mantia, T., 2017. Agricultural land abandonment in Mediterranean environment
592 provides ecosystem services via soil carbon sequestration. *Sci. Total Environ.*
593 <https://doi.org/10.1016/j.scitotenv.2016.10.123>

594 Osawa, T., Kadoya, T., Kohyama, K., 2015. 5- and 10-km mesh datasets of agricultural land
595 use based on governmental statistics for 1970–2005. *Ecol. Res.*
596 <https://doi.org/10.1007/s11284-015-1290-2>

597 Pazúr, R., Lieskovský, J., Feranec, J., Oľahel', J., 2014. Spatial determinants of abandonment
598 of large-scale arable lands and managed grasslands in Slovakia during the periods of
599 post-socialist transition and European Union accession. *Appl. Geogr.* 54, 118–128.
600 <https://doi.org/10.1016/j.apgeog.2014.07.014>

601 Plieninger, T., Hui, C., Gaertner, M., Huntsinger, L., 2014. The impact of land abandonment
602 on species richness and abundance in the Mediterranean Basin: A meta-analysis. *PLoS*
603 *One*. <https://doi.org/10.1371/journal.pone.0098355>

604 Pointereau, P., Coulon, F., Girard, P., Lambotte, M., Stuczynski, T., Sánchez Ortega, V., Del
605 Rio, A., 2008. Analysis of the Driving Forces behind Farmland Abandonment and the
606 Extent and Location of Agricultural Areas that are Actually Abandoned or are in Risk to
607 be Abandoned, JCR Scientific and Technical reports.
608 <https://doi.org/10.13140/RG.2.1.2467.7849>

609 Queiroz, C., Beilin, R., Folke, C., Lindborg, R., 2014. Farmland abandonment: Threat or
610 opportunity for biodiversity conservation? A global review. *Front. Ecol. Environ.*
611 <https://doi.org/10.1890/120348>

612 Ramankutty, N., Foley, J.A., 1999. Estimating historical changes in land cover North
 613 American croplands from 1850 to 1992. *Glob. Ecol. Biogeogr.*
 614 <https://doi.org/10.1046/j.1365-2699.1999.00141.x>

615 Ramankutty, N., Foley, J.A., 1999. Estimating historical changes in global land cover:
 616 Croplands from 1700 to 1992. *Global Biogeochem. Cycles.*
 617 <https://doi.org/10.1029/1999GB900046>

618 Rodrigo-Comino, J., Martinez-Hernandez, C., Iserloh, T., Cerda, A., 2018. Contrasted Impact
 619 of Land Abandonment on Soil Erosion in Mediterranean Agriculture Fields. *Pedosphere.*
 620 [https://doi.org/10.1016/S1002-0160\(17\)60441-7](https://doi.org/10.1016/S1002-0160(17)60441-7)

621 Romero-Diaz, A., Belmonte-Serrato, F., Ruiz-Sinoga, J.D., 2010. The geomorphic impact of
 622 afforestations on soil erosion in southeast Spain. *L. Degrad. Dev.*
 623 <https://doi.org/10.1002/ldr.946>

624 Rosstat, 2010. Regions of Russia. Socio-Economic Measures (Regiony Rossii. Sotsio-
 625 ekonomicheskie Pokazateli) (Moscow: Russian Federal Service of State Statistics).

626 Schierhorn, F., Müller, D., Beringer, T., Prishchepov, A. V., Kuemmerle, T., Balman, A.,
 627 2013. Post-Soviet cropland abandonment and carbon sequestration in European Russia,
 628 Ukraine, and Belarus. *Global Biogeochem. Cycles.*
 629 <https://doi.org/10.1002/2013GB004654>

630 Schneider, C.A., Rasband, W.S., Eliceiri, K.W., 2012. NIH Image to ImageJ: 25 years of
 631 image analysis. *Nat. Methods* 9, 671–675. <https://doi.org/10.1038/nmeth.2089>

632 Simms, A.D., Woodroffe, C., Jones, B.G., Heijnis, H., Mann, R.A., Harrison, J., 2008. Use of
 633 ^{210}Pb and ^{137}Cs to simultaneously constrain ages and sources of post-dam sediments in
 634 the Cordeaux reservoir, Sydney, Australia. *J. Environ. Radioact.* 99, 1111–1120.

<https://doi.org/10.1016/j.jenvrad.2008.01.002>

Van Rompaey, A., Krasa, J., Dostal, T., 2007. Modelling the impact of land cover changes in the Czech Republic on sediment delivery. *Land use policy* 24, 576–583.

<https://doi.org/10.1016/j.landusepol.2005.10.003>

Warren, J., Gilbert, R.O., 1988. *Statistical Methods for Environmental Pollution Monitoring. Technometrics.* <https://doi.org/10.2307/1270090>

Figures

Fig. 1: (a) Localization map of the study sites within the Loire River basin (PG= Prugnolas site, MA = Malaguet site), (b) detailed map of the Prugnolas catchment, (c) detailed map of the Malaguet catchment, (d), Prugnolas pond characteristics and core sampling location, (e) Malaguet lake characteristics and core sampling location.

Fig. 2: Evolution of the population in the Prugnolas and Malaguet catchments during the 20th century

Fig. 3: Evolution of the main land uses between 1948 and 2010 in the Prugnolas and Malaguet catchments based on the analysis of aerial images and agricultural census data. Grey areas correspond to the afforestation periods.

Fig. 4: Illustration of the spatial pattern of land use change in the Prugnolas catchment between 1950 and 2000. Land use was estimated from on digitized aerial images.

Fig. 5: Age model of the 43-MA-1703 core (Malaguet lake) based on the fallout radionuclide activity measurements.

Fig. 6: Evolution of the mass accumulation rate and the terrigenous material input fraction estimated from the changes in K/Ca ratio based on XRF measurements in the sediment core collected in the Prugnolas pond.

Fig. 7: Evolution of the mass accumulation rate and the terrigenous material input fraction estimated from the changes in K/Ca ratio based on XRF measurements in the sediment core collected in the Malaguet lake.

Fig. 8: Comparison between average Mass Accumulation Rate, evolution of population and proportion of arable land for the Malaguet and Prugnolas catchment

Supplementary material:

Table 1: Evolution of land use in the Prugnolas catchment between 1950 and 2010.

*correspond to land use estimated by the analysis of aerial images

684 Table 2: Evolution of land use in the Malaguet catchment between 1950 and 2010

685 *correspond to land use estimated by the analysis aerial imageries

686

Table 1
[Click here to download Tables: table1.docx](#)

	2010	2000	2000*	1988	1979	1979*	1972*	1970	1955	1950*
Arable land (%)	16	13	12	18	20	26		20	47	68
Cropland (%)	0,4	0,7	0,9	1,7	2,4	3,6		3,3	5,5	7,3
Grassland (%)	16	13	11	16	17	23		17	42	61
Permanent (%)	14	10	-	15	16	-		13	-	-
temporary (%)	2	2	-	1	2	-		3	-	-
Forest (%)	82	85	86	80	78	72		78	51	30
Other	2	2	2	2	2	2		2	2	2
Urban area (%)	2	2	2	2	1	1		1	1	1
Water body (%)	0,5	0,5	0,5	0,5	0,5	0,5		0,5	0,5	0,5

Table 2
[Click here to download Tables: table 2.docx](#)

	2010	2000	1995*	1988	1979	1977*	1970	1967*	1955*	1948*
Arable land (%)	15	18	21	23	28	33	38	39	44	45
Cropland (%)	2	3	5	5	7	8	9	13	14	13
Grassland (%)	13	14	17	18	19	25	28	26	29	33
Forest (%)	71	69	65	64	62	55	51	50	45	43
Other	13	13	13	13	12	12	12	12	12	12
Urban area (%)	6	6	6	6	6	6	5	5	5	5
Water body (%)	7	7	7	7	7	7	6	6	6	6

Fig. 1

[Click here to download high resolution image](#)

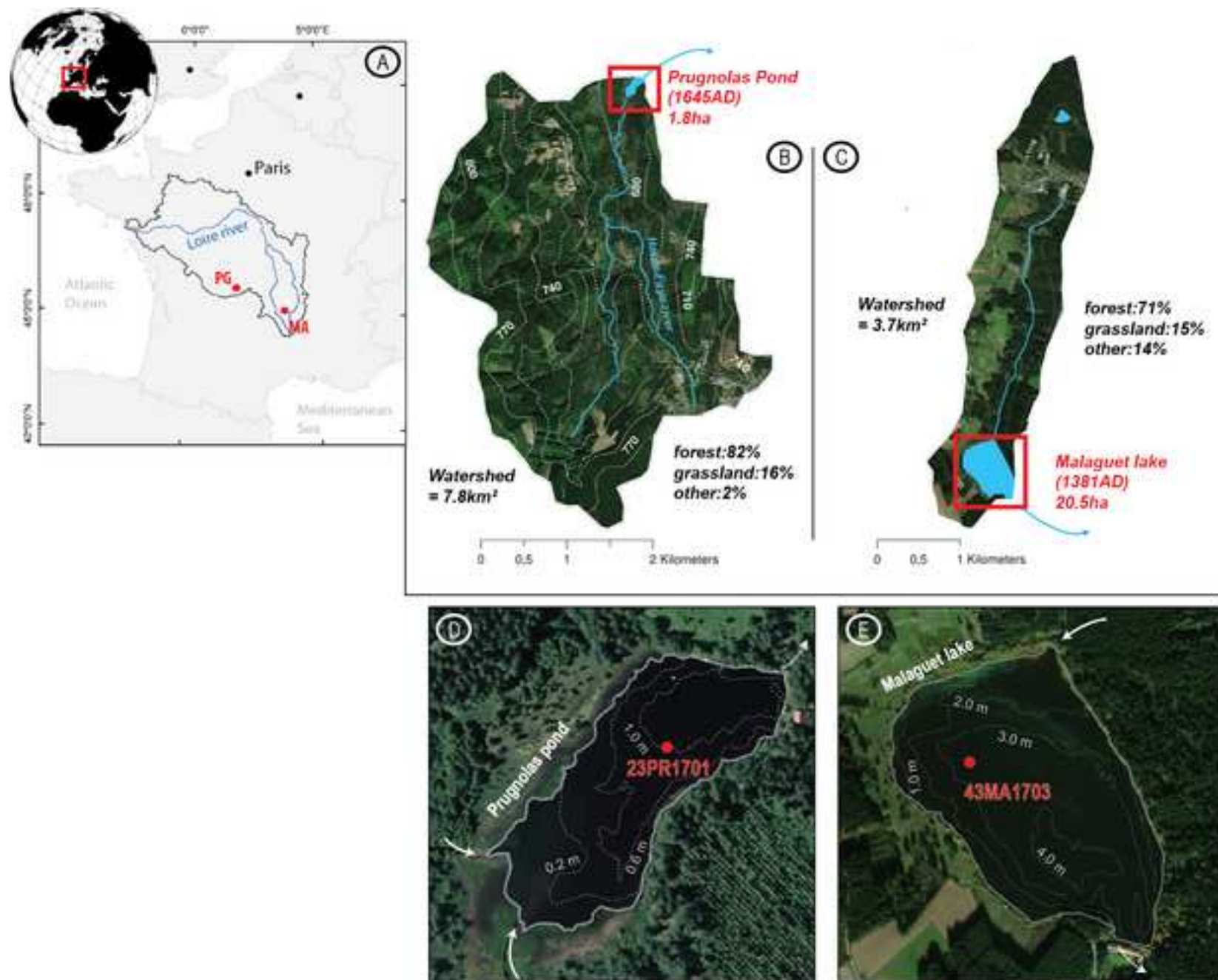


Fig. 2

[Click here to download high resolution image](#)

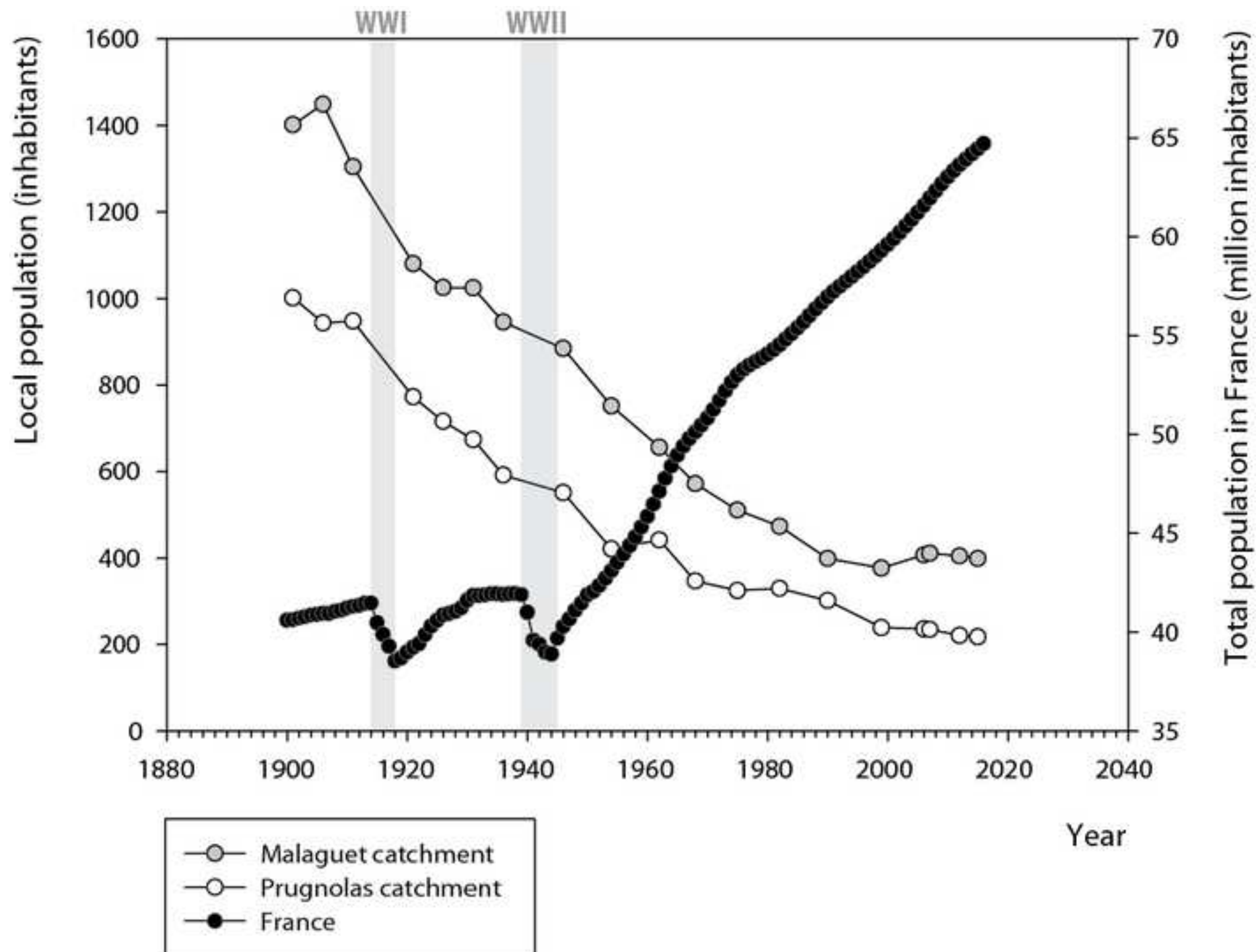


Fig. 3

[Click here to download high resolution image](#)

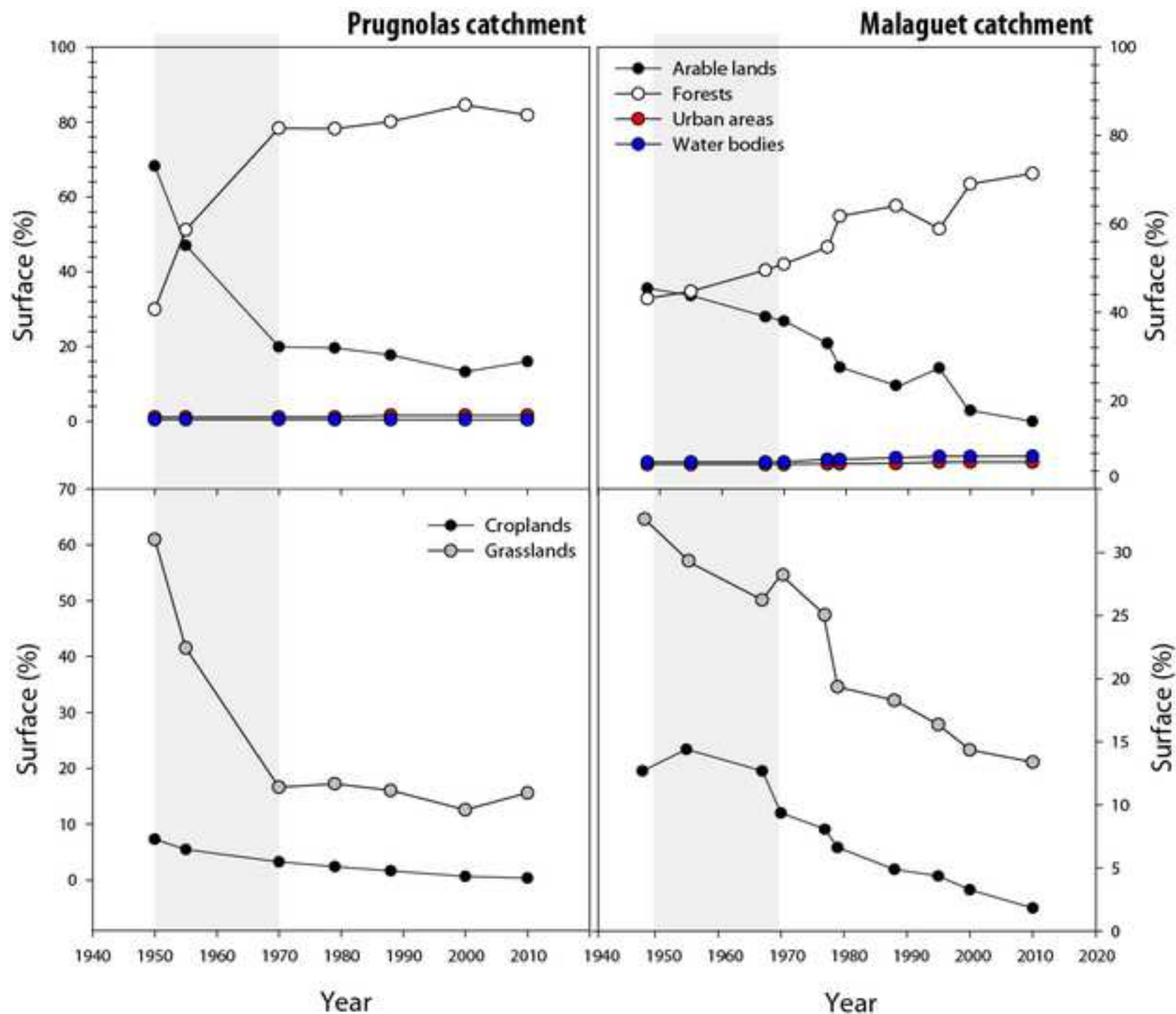


Fig. 4

[Click here to download high resolution image](#)

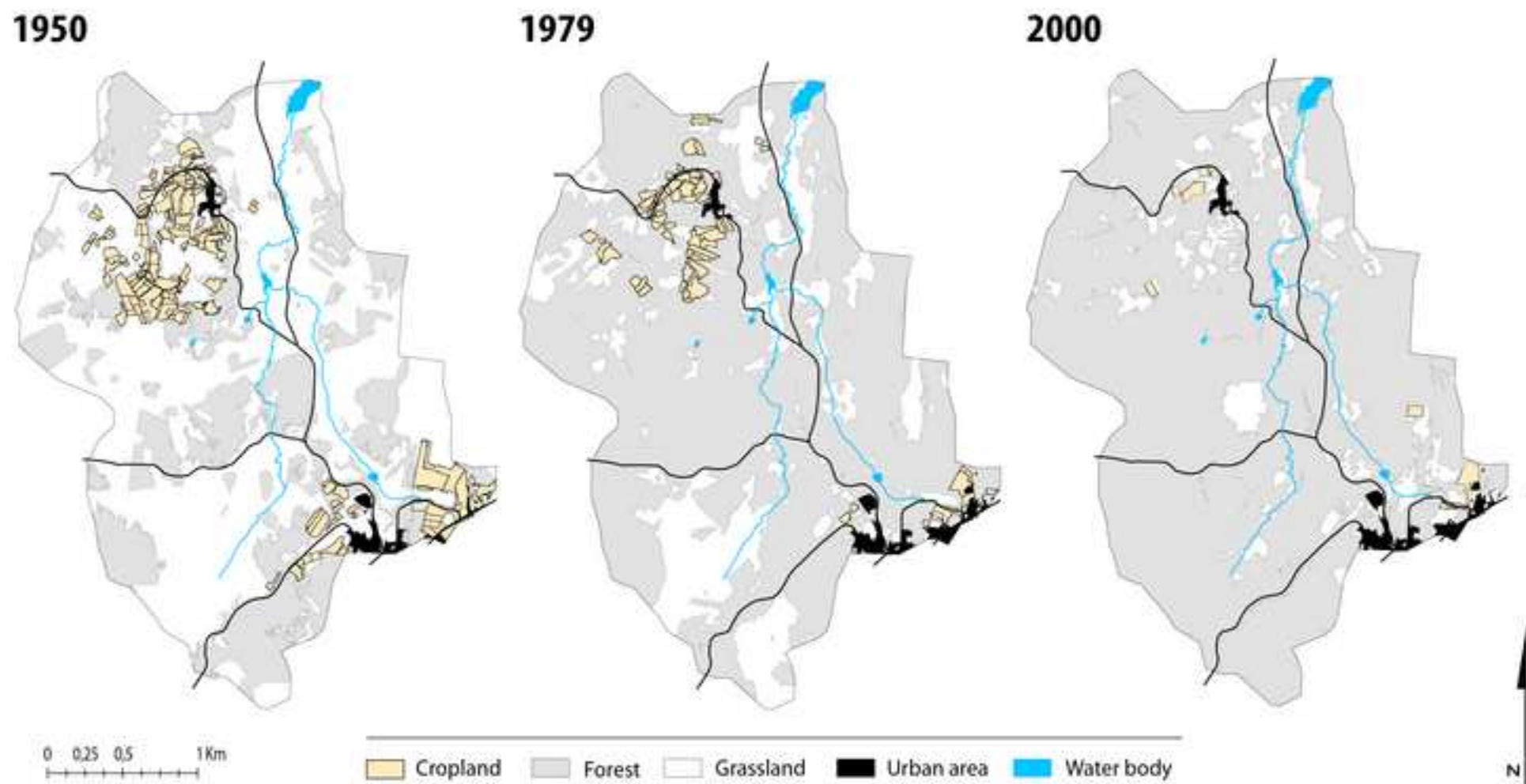


Fig. 5

[Click here to download high resolution image](#)

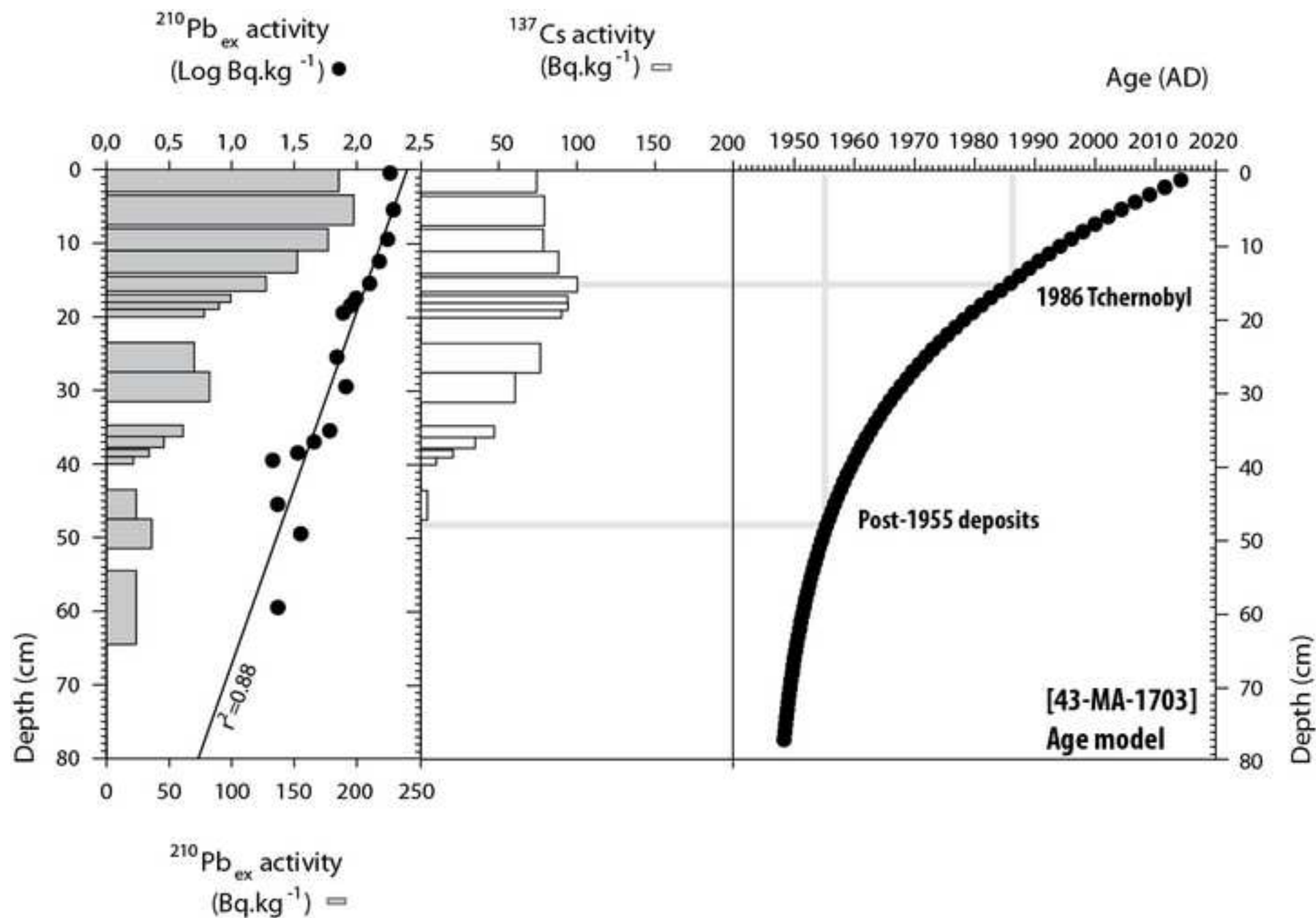


Fig. 6

[Click here to download high resolution image](#)

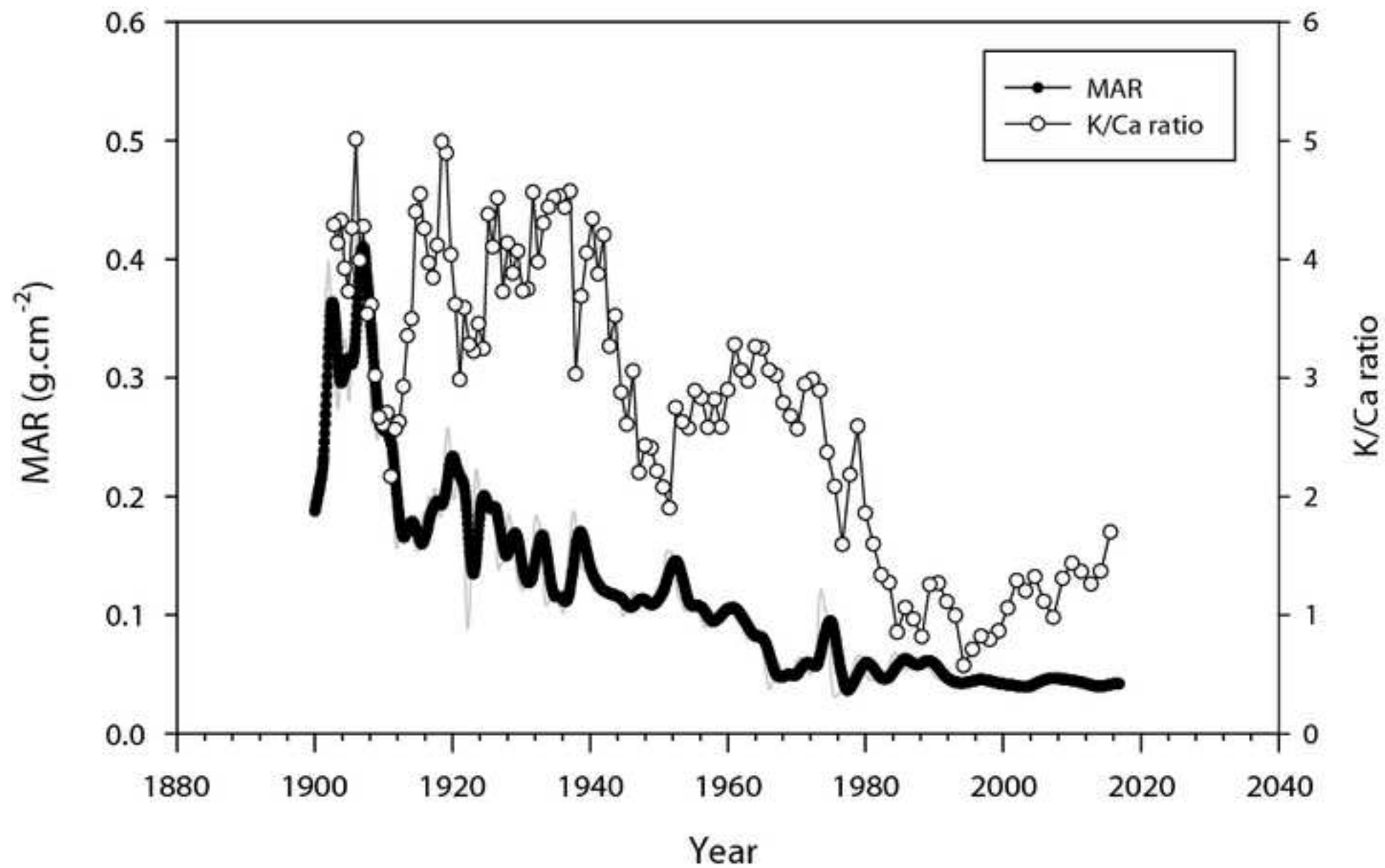


Fig. 7

[Click here to download high resolution image](#)

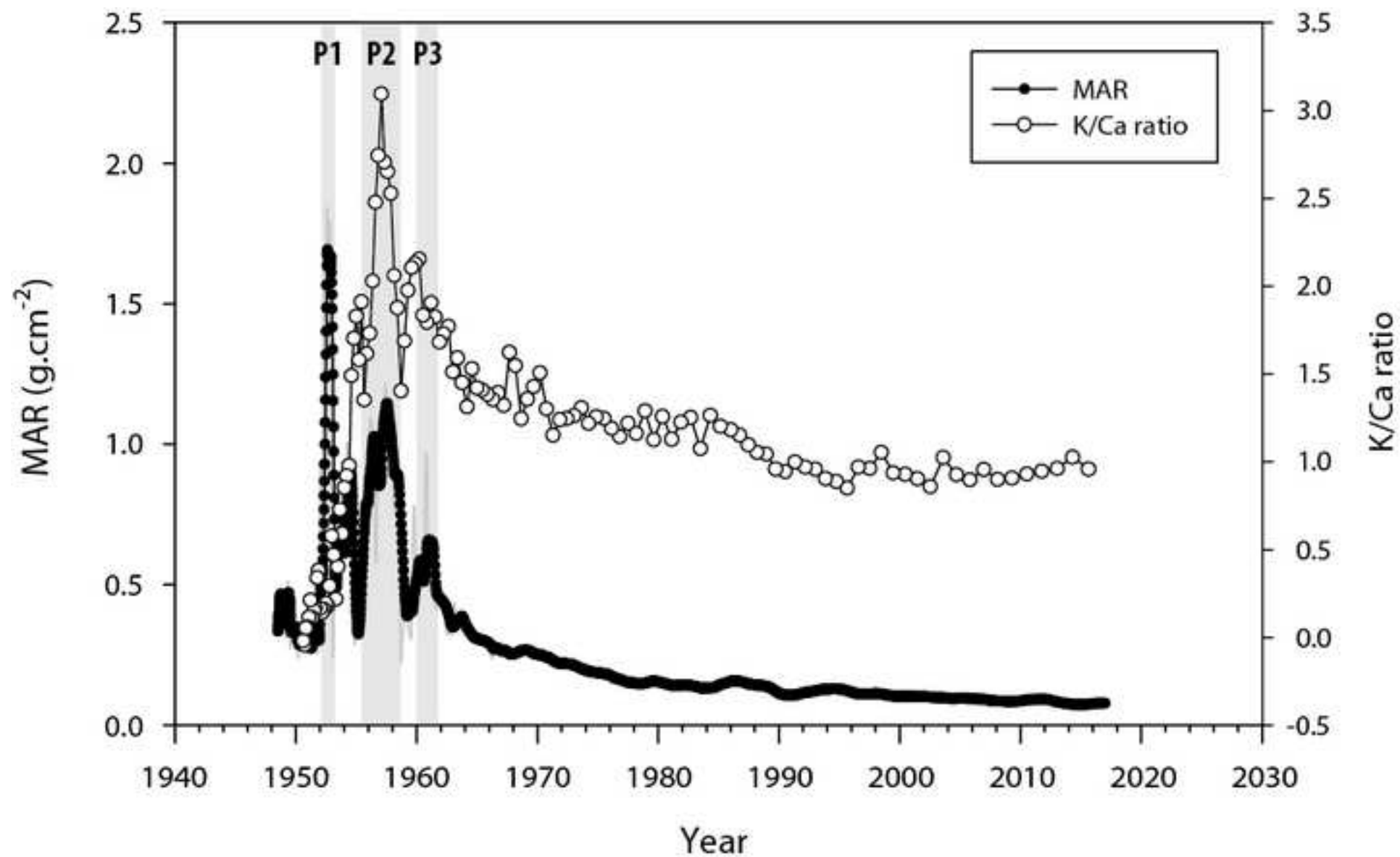


Fig. 8
[Click here to download high resolution image](#)

